

Thermodynamic Properties of Aqueous HClO₄ to 373 K and at Low Pressure: A Comprehensive Pitzer Ion-Interaction Model

Charles S. Oakes* and Dhanpat Rai

Battelle, Pacific Northwest National Laboratory, Actinide and Trace Metal Geochemistry, P7-50, Richland, Washington 99352

We present a Pitzer ion-interaction model fit to most of the available isopiestic, dilution enthalpy, heat capacity, and volumetric data for HClO₄(aq). Osmotic and activity coefficients are accurately reproduced for molalities between infinite dilution and 8 mol kg⁻¹ at 298 K. Isopiestic data at temperatures other than 298 K do not appear to be reliable. The dilution enthalpy data at 298 K are also reproducible to 8 mol kg⁻¹; consequently, HClO₄(aq) activities may be calculated to 8 mol kg⁻¹ at 298 K and at somewhat higher or lower temperatures with only minor losses in confidence. Heat capacity data do not extend beyond 1.7 mol kg⁻¹ at 298 K and 1.0 mol kg⁻¹ at $T > 328$ K, and interlaboratory agreement is poor. Consequently, activity coefficients and thermal properties may only be calculated to about 1 mol kg⁻¹ at 373 K. There are numerous volumetric data for molalities between 0.02 and 18 mol kg⁻¹ and at 298 K; however, there are large variances between datasets at $m > 5$ mol kg⁻¹. Volumetric data at $T > 348$ K are limited to one study and $m < 1$ mol kg⁻¹. The volumetric form of the model is simple but due to disagreement between datasets is considered to have large uncertainties.

Introduction

Perchloric acid is an important industrial acid and is frequently used in chemical research as a supporting electrolyte due to the weak complexing characteristics of the ClO₄⁻ anion. Use of HClO₄(aq) is particularly common in actinide solubility and speciation studies. As temperatures in nuclear waste repositories and processing environments may significantly exceed 298 K and activity coefficient models for HClO₄(aq)^{1–3} are limited to 298 K or near 298 K, there is a need for a model which reproduces HClO₄ activities over wide ranges of molality and temperature.

Our own interest in HClO₄(aq) stems from a need for the standard state chemical potential for Nd³⁺(aq) as a function of temperature. This need arises from the use of neodymium as an analogue for trivalent actinides. As the only neodymium salt for which the necessary thermodynamic data exist is Nd[ClO₄]₃, temperature dependencies for the infinite dilution heat capacities ($C_{p,\phi}^\infty$) of HClO₄(aq) and Nd[ClO₄]₃(aq) are needed (if the convention of zero valued standard state properties for H⁺ is assumed). An additional need arises from the fact that most of the Nd[ClO₄]₃(aq) data are from the mixed system H⁺ + Nd³⁺ + ClO₄⁻. We will present a temperature-dependent Pitzer ion-interaction model for Nd[ClO₄]₃(aq) in a subsequent paper.

Two groups have measured HClO₄(aq) heat capacities at $T = 298$ K and fit Pitzer ion-interaction or Born models to their datasets,^{4–7} thus, in principle, allowing us to calculate the requisite $C_{p,\phi}^\infty$ values without any further analysis. However, intercomparison of the former datasets as well as comparison with others^{8,9} shows substantial scattering between studies and within individual datasets. In addition, comparison of $C_{p,\phi}^\infty$ values from the cited studies with values estimated from additivity of standard

states shows large discrepancies. This study addresses these discrepancies and presents a Pitzer ion-interaction model which reproduces the available HClO₄(aq) activity coefficient, enthalpy, heat capacity, and volumetric data from 298 K to 373 K and at pressures near 0.1 MPa.

Thermodynamic Model

A Pitzer ion-interaction model^{10,11} was fit to the data from the sources^{4,5,7,9,12–24} listed in Table 1. The equation for a system containing a single, fully dissociated 1:1 electrolyte is

$$G^{\text{xs}}/(w_w RT) = f(I) + 2m^2[B_{\text{MX}} + \frac{1}{2}ZC_{\text{MX}}] \quad (1)$$

where $w_w = 1$ kg of H₂O, $R = 8.314 41$ J mol⁻¹ K⁻¹, m is molality, and B_{MX} and C_{MX} are the second and third virial coefficients. The Debye–Hückel term is

$$f(I) = -4IA_\phi \ln(1 + b\sqrt{I})/b \quad (2)$$

where b has the universal value of 1.2 kg^{-1/2} mol^{-1/2}, I is ionic strength, and A_ϕ is a function of water density²⁵ and dielectric constant.²⁶ The quantity $Z = \sum_i m_i |z_i|$, where z_i is the charge on each ion. B_{MX} is given an ionic strength dependency of the form

$$B_{\text{MX}} = \beta_{\text{MX}}^{(0)} + \beta_{\text{MX}}^{(1)}g(x) \quad (3)$$

$$g(x) = 2[1 - (1 + x) \exp(-x)]/x^2 \quad (4)$$

where $x = \alpha_1 \sqrt{I}$ and $\alpha_1 = 2.0$ kg^{1/2} mol^{-1/2}.

Differentiation of eq 1 with respect to n_i , n_w , p , or T and addition of standard state properties where appropriate yield the ionic activity coefficients (γ_i), osmotic coefficient (ϕ), and apparent molar volume (V_ϕ), enthalpy (L_ϕ), and heat capacity ($C_{p,\phi}$).

* Now at Ceramics and Materials Engineering, Rutgers University, Piscataway, NJ 08854. E-mail: OakesCS@rci.rutgers.edu.

Table 1. Thermodynamic Property, Range of Experimental Conditions, and Source for Data Used in This Study

property	T/T_0^a	m/m_0^b	n^c	σ^d	ref
ϕ	298	0.1–11.9	12	0.023	12
ϕ	298	0.1–15.7	5, ^f 26 ^g	0.007, ^f 0.003 ^g	13
ϕ	283–313	0.3–14.0	(13)	NA	14
ϕ	298	0.56–8.3	15, ^f 9 ^g	0.004, ^f 0.003 ^g	15
ϕ	298	6.6–19.7	1 ^f	NA	16
ϕ	298	1.19–9.8	11 ^f	0.005 ^f	17
ϕ	323	1.5–24.0	10	0.162	18
ϕ	298	0.05–1.1	6 ^g	0.001 ^g	19
ϕ	298	0.10–4.5	14 ^g	0.004 ^g	20
L_ϕ	298	0.005–15	48	19	21
$C_{p,\phi}$	288–328	0.05–0.22	(30)	NA	8
$C_{p,\phi}$	298	0.05–0.37	9	1.8	9
$C_{p,\phi}$	298	0.09–1.06	9	1.8	4
$C_{p,\phi}$	283–328	0.18–1.08	8	5.9, 3.2, 4.6	5
$C_{p,\phi}$	298–373	0.10–1.61 ^e	20, 7, 7, 7, 7	3.6, 4.4, 3.8, 2.3, 1.9	7
V_ϕ	298	0.10–11.9	15	0.23	12
V_ϕ	298–303	0.10–18.5	22, 4	0.09, 0.03	22
V_ϕ	298–348	0.24–3.13	12	0.07, 0.09, 0.05, 0.06, 0.07, 0.29	23
V_ϕ	298	0.09–1.06	9	0.21	4
V_ϕ	283–328	0.18–1.08	8, 9, 8	0.23, 0.59, 0.37	5
V_ϕ	293–308	0.10–4.35	16	0.14, 0.17, 4.3, 9.4	24
V_ϕ	296–372	0.10–1.61 ^e	20, 7, 7, 7, 7	0.42, 0.53, 0.41, 0.36, 0.31	7

^a $T_0 = 1$ K. ^b $m_0 = 1.0$ mol kg⁻¹. ^c $n =$ number of datum in dataset for $m \leq 8$ mol kg⁻¹. ^d $\sigma =$ rms error calculated for each dataset at $m \leq 8$ mol kg⁻¹. The dimensions of σ are the units of the corresponding property type (see figures). Where one n is listed with multiple values of σ , each dataset within the study contains n points. ^e At $T > 298$ K, $m_{\max} = 0.6$ mol kg⁻¹. ^f H₂SO₄(aq) std. ^g NaCl(aq) std.

The osmotic coefficient expression for this system is

$$\phi - 1 = (1/m)[-A_\phi I^{3/2}/(1 + b\sqrt{I}) + m^2(B_{MX}^\phi + ZC_{MX}^\phi)] \quad (5)$$

where

$$B_{MX}^\phi = \beta_{MX}^{(0)} + \beta_{MX}^{(1)} \exp(-x) \quad (6)$$

and

$$C_{MX}^\phi = C_{MX} \quad (7)$$

Note that, due to our adoption of the equivalence in form between B_{MX}^ϕ and C_{MX}^ϕ , C_{MX}^ϕ in eq 7 is different from Pitzer's¹⁰ by a factor of $2|z_M z_X|^{1/2}$; for example, $C_{MX}^\phi = C_{MX,Pitzer}^\phi/[2|z_M z_X|^{1/2}]$.

The generalized activity coefficient equations for specific cations (M) and anions (X), respectively, are

$$\ln \gamma_M = z_M^2 F + \sum_a m_a (2B_{Ma} + ZC_{Ma}) + z_M \sum_c \sum_a m_c m_a C_{ca} \quad (8)$$

and

$$\ln \gamma_X = z_X^2 F + \sum_c m_c (2B_{cX} + ZC_{cX}) + |z_X| \sum_c \sum_a m_c m_a C_{ca} \quad (9)$$

where

$$F = f' + \sum_c \sum_a m_c m_a B_{ca} + 1/2 \sum_c \sum_a m_c m_a ZC_{ca} \quad (10)$$

$$f' = -A_\phi [I^{1/2}/(1 + bI^{1/2}) + 2 \ln(1 + bI^{1/2})/b] \quad (11)$$

$$B_{MX} = \beta_{MX}^{(1)} g'(x) \quad (12)$$

$$g'(x) = -I^{-1}[g(x) - \exp(-x)] \quad (13)$$

and where mixing effects between ions of like sign or

neutral species are ignored. The summations over c and a pertain to all cations and anions, respectively, in the system. Since the system of interest is a 1:1 electrolyte and no other salts are considered, the summations in eqs 8–10 are unnecessary and consequently have been omitted in the subsequent equations for the derivative properties. For simple systems in which aqueous phase speciation reactions are not considered, the mean ionic activity coefficient (γ_\pm) is commonly used and is defined as

$$\ln \gamma_\pm = (\nu_M \ln \gamma_M + \nu_X \ln \gamma_X)/\nu \quad (14)$$

where ν is the sum of cations (ν_M) and anions (ν_X) in the electrolyte formula unit. The notations used above are identical to those used by Pitzer.¹¹

The model equation for the relative enthalpy²⁷ (L) is

$$L/(w_w RT^2) = -\frac{\partial f(I)}{\partial T} - 2m^2[B_{MX}^L + 1/2 ZC_{MX}^L] \quad (15)$$

$$\frac{\partial f(I)}{\partial T} = \frac{A_L}{bRT^2} I \ln(1 + b\sqrt{I}) \quad (16)$$

and

$$A_L = 4RT^2 \left(\frac{\partial A_\phi}{\partial T} \right)_{p,I}, \quad B_{MX}^L = \left(\frac{\partial B_{MX}}{\partial T} \right)_{p,I} \quad \text{and} \quad C_{MX}^L = \left(\frac{\partial C_{MX}}{\partial T} \right)_{p,I} \quad (17a-c)$$

The apparent molar enthalpy is $L_\phi = L/n_2$, where n_2 is the number of moles of solute.

The apparent molar heat capacity is given by²⁷

$$C_{p,\phi}/(w_w RT^2) = C_{p,\phi}^\infty/(w_w RT^2) + \frac{1}{n_2} \left[\frac{2}{T} \frac{\partial f(I)}{\partial T} + \frac{\partial^2 f(I)}{\partial T^2} - 2m^2[B_{MX}^J + 1/2 ZC_{MX}^J] \right] \quad (18)$$

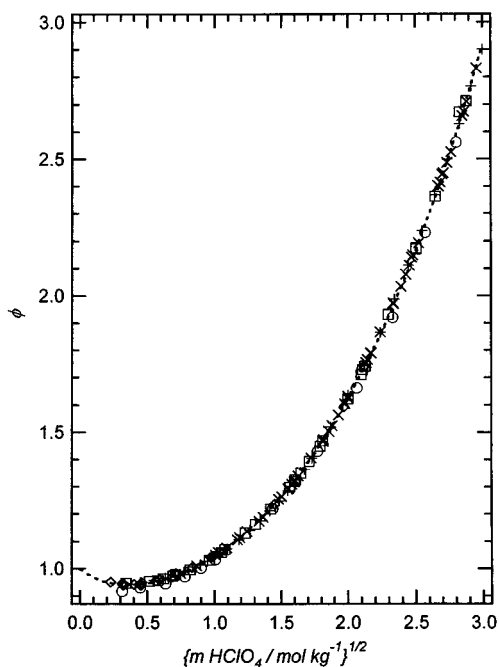


Figure 1. Osmotic coefficient data from the literature at 298.15 K: (○) ref 12; (□) ref 13; (+) ref 14; (×) refs 15, 17, and 50; (◇) refs 19 and 20; (···) calculated from eq 5.

where

$$\frac{2}{T} \frac{\partial f(I)}{\partial T} + \frac{\partial^2 f(I)}{\partial T^2} = \frac{A_J}{bRT^2} I \ln(1 + b\sqrt{I}) \quad (19)$$

$$A_J = \left(\frac{\partial A_L}{\partial T} \right)_{p,I}, \quad B_{MX}^J = \left(\frac{\partial^2 B_{MX}}{\partial T^2} + \frac{2}{T} \frac{\partial B_{MX}}{\partial T} \right)_{p,I}, \quad \text{and} \\ C_{MX}^J = \left(\frac{\partial^2 C_{MX}}{\partial T^2} + \frac{2}{T} \frac{\partial C_{MX}}{\partial T} \right)_{p,I} \quad (20a-c)$$

The corresponding equation for V_ϕ is¹¹

$$V_\phi / (w_w RT) = V_\phi^0 / (w_w RT) + \frac{1}{n_2} \left[\frac{\partial f(I)}{\partial p} + 2m^2 [B_{MX}^V + 1/2 ZC_{MX}^V] \right] \quad (21)$$

where

$$\frac{\partial f(I)}{\partial p} = \frac{A_V}{bRT} I \ln(1 + b\sqrt{I}) \quad (22)$$

$$A_V = \left(\frac{\partial A_\phi}{\partial p} \right)_{T,I}, \quad B_{MX}^V = \left(\frac{\partial B_{MX}}{\partial p} \right)_{T,I}, \quad \text{and} \\ C_{MX}^V = \left(\frac{\partial C_{MX}}{\partial p} \right)_{T,I} \quad (23a-c)$$

Treatment of the Data

The model was simultaneously fit to all of the experimental data from the sources in Table 1 using the data forms ϕ , L_ϕ , $C_{p,\phi}$, and V_ϕ . As well as identifying sources of datatypes, Table 1 includes molality and temperature ranges, number of datum in each dataset, and the root-mean-square (rms) errors between the model and each dataset.

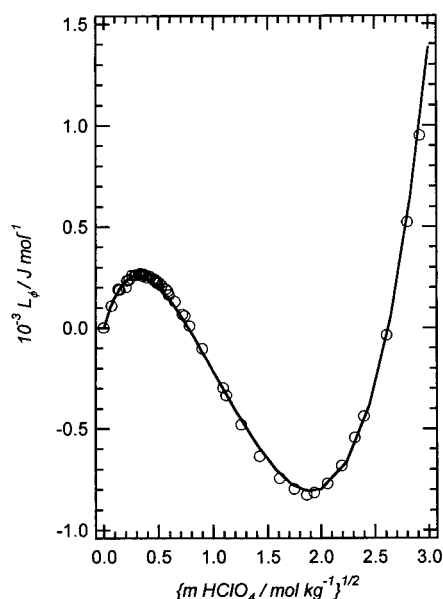


Figure 2. Apparent molar enthalpy data (○)²¹ at 298 K and 0.1 MPa; (—) calculated from eq 15.

The isopiestic data at 298 K are shown in Figure 1. Isopiestic or vapor-pressure measurements have also been conducted at 283 K, 313 K, and 323 K and to high molalities; however, unsmoothed data are not presented.^{14,18} Because Haase et al.'s smoothed ϕ 's at 298 K are in good agreement with the other data, we attempted to recalculate and fit their 283 K and 313 K isopiestic measurements, which are reported as $\ln \gamma_\pm$'s. Unfortunately, the lowest molality in their tabulation is 0.3 *m*; consequently, any function for γ_\pm between infinite dilution and 0.3 *m* is unconstrained and the Gibbs–Duhem transformation results in unreasonable values of ϕ . For those sources in which original isopiestic molalities are presented, the data were recalculated using modern models for the isopiestic coefficients of the corresponding standard solutions, for example, $H_2SO_4(aq)$ ²⁸ and $NaCl(aq)$.²⁹

Dilution enthalpy data for this system are limited to 298 K and 0.1 MPa.²¹ These data were fit using the tabulated values of L_ϕ from the original source (Figure 2).

Values of $C_{p,\phi}$ were used as published in the original sources.^{4,5,7,9} Differences resulting from recalculation using a common model for water would be substantially smaller than the inter- and intralaboratory precision of the data. Hovey's^{4,5} $C_{p,\phi}$ data are systematically more positive than Lemire's⁷ by 6 to 8 $J mol^{-1} K^{-1}$ (Figure 3). Lemire conducted replicate measures at fixed molalities, and from these their reproducibility appears to be roughly independent of temperature and to be about $\pm 0.5 J mol^{-1} K^{-1}$. Hovey^{4,5} estimated uncertainties in $C_{p,\phi}^\infty$ ($\pm 0.7 J mol^{-1} K^{-1}$ at 298 K to $\pm 2.0 J mol^{-1} K^{-1}$ at 328 K). It is reasonable to assume that their measurement errors were not larger. Lemire's measurements were conducted at 0.5 MPa versus 0.1 MPa for the Hovey and Singh measurements. This pressure difference might result in as much as 1 $J mol^{-1} K^{-1}$ difference for a given molality. As the offset between the Lemire and Hovey or Singh datasets is roughly twice the magnitude of the combined uncertainties, it appears that there is a systematic problem either with Lemire's calorimeter or with both the Hovey and Singh calorimeters. Lemire calibrated their instrument with $NaCl(aq)$ at each experimental temperature while Hovey calibrated with water only at 298 K and assumed that heat losses were independent of temperature. It could be argued that the

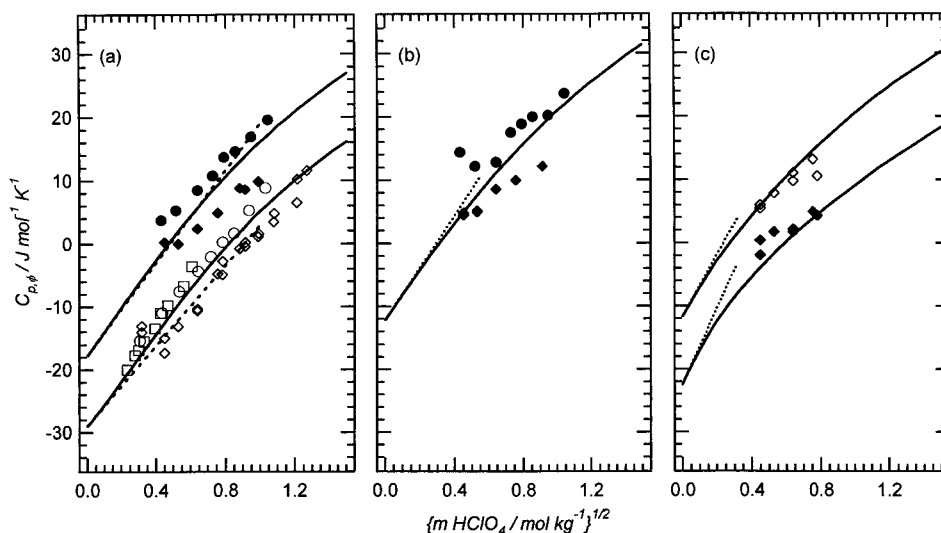


Figure 3. Apparent molar heat capacity data at (a) 298 K [\square] ref 9; (\circ) ref 4; (\diamond) ref 7 and 313 K [\bullet] ref 5; (\blacklozenge) ref 7], (b) 328 K [\bullet] ref 5; (\blacklozenge) ref 7], and (c) 348 K [\diamond] ref 7 and 373 K [\blacklozenge] ref 7: (—) calculated from eq 18; (···) Debye–Hückel limiting law slope.

Lemire data are likely to be more accurate on the basis of a more thorough procedure. However, since the Singh and Hovey data are in good agreement, a more substantive reason is required to bias the model. If there is a problem with the Lemire dataset, then our model's temperature dependence above 328 K will be in error, as the model is guided only by Lemire's data at the higher temperatures. Additional data are available;⁸ however, these data vary widely from the other datasets, for example, by at least 5 J mol⁻¹ K⁻¹ at 298 K and by at least 35 J mol⁻¹ K⁻¹ at 328 K. These differences increase with molality as well as with temperature.

Like the heat capacity data, and for the same reason, values of V_ϕ were used as originally published^{4,5,7,12,22–24} unless the data were only published as densities, in which case values of V_ϕ were calculated using the Hill equation of state for water.²⁵ Lemire et al.'s⁷ volumetric measurements were also made at 0.5 MPa versus 0.1 MPa for all other measurements.

As the published heat capacity and volumetric data for HClO₄(aq) tend to be imprecise (cf. Figures 3 and 4, respectively) we investigated the option of constraining $V_\phi^\infty(\text{HClO}_4)$ and $C_{p,\phi}^\infty(\text{HClO}_4)$ through additivity of standard state heat capacities or volumes using aqueous M²⁺Cl₂, M²⁺[ClO₄]₂, and HCl. For $C_{p,\phi}^\infty(\text{HCl})$ we used Holmes et al.,³⁰ and for $V_\phi^\infty(\text{HCl})$, Sharygin and Wood.³¹ Other strong acid [HX] and M[ClO₄]₂–MX pairs could have been used; however, HCl(aq) is probably the best known nonassociating acid for the temperature range considered by this study. Consequently, little would have been gained by pursuing additional systems. Our model infinite dilution heat capacities and volumes and those derived from additivity are shown in Figure 5. Infinite dilution properties derived from additivity were included in the fit; however, these values were allowed very little influence on the model.

Aside from the cited source for HCl(aq), values of $C_{p,\phi}^\infty(\text{HClO}_4)$ were estimated from the following systems: NaCl(aq);²⁹ NaClO₄(aq);^{9,32,33} KCl(aq);³⁴ and KClO₄(aq).³⁵ As pointed out by Lemire et al.,⁷ values of $C_{p,\phi}^\infty(\text{KClO}_4)$ could contain large errors due to the very limited molality range over which data exist for this salt. The only values of $C_{p,\phi}^\infty(\text{KClO}_4)$ at $T > 298$ K are those from Mastroianni and Criss,³² which are based on $C_p^\infty(\text{NaClO}_4, \text{solid})$ ³⁶ and

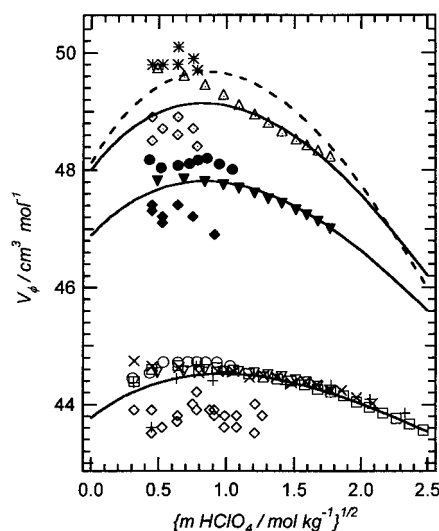


Figure 4. Apparent molar volume data at 298 K [\circ] ref 4; (\diamond) ref 7; (+) ref 12; (\square) ref 22; (∇) ref 23; (\times) ref 24]; 328 K [\bullet] ref 5; (\blacklozenge) ref 7; (\blacktriangledown) ref 23]; 348 K [(tilted square dotted) ref 7; (triangle open dotted) ref 23]; 372 K [(*) ref 7]; 298, 328, and 348 K (—); and 373 K as calculated from eq 21 (---).

their enthalpy of solution measurements for NaClO₄(solid). The only other non-actinide or -lanthanide chloride–perchlorate pairs for which relevant heat capacity data exist are those for Ni[ClO₄]₂(aq)³⁷ and NiCl₂(aq).^{38–40} At other than 298 K the measurements for the latter two systems were made at substantially different pressures and thus were not used.

Values of $V_\phi^\infty(\text{HClO}_4)$ can be estimated from NH₄Cl(aq) and NH₄ClO₄(aq);⁴¹ KCl(aq);^{42,43} KClO₄(aq);³⁵ NiCl₂(aq);^{38,39,44,45} and Ni[ClO₄]₂(aq).^{37,45} Values of $V_\phi^\infty(\text{HClO}_4)$ using NH₄Cl(aq) and NH₄ClO₄(aq) are considerably different from values supported by the HClO₄(aq) data and from additivity using other systems—most likely due to uncorrected hydrolysis effects. Values of $V_\phi^\infty(\text{HClO}_4)$ from most of the other sources are in reasonably good agreement below about 308 K but diverge rapidly at higher temperatures. Somewhat surprisingly, there do not appear to be any unsmoothed volumetric data for NaClO₄(aq) at $T > 298$ K.

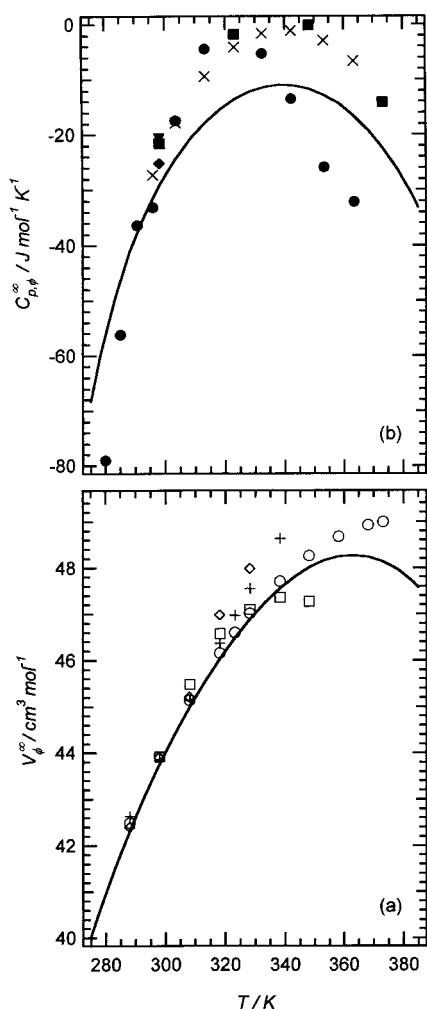


Figure 5. Apparent molar volumes (a) and heat capacities (b) at infinite dilution from additivity as functions of temperature. Aside from HCl(aq) properties,^{30,31} sources and chemical combinations are as follows: (a) (○) refs 35 and 43; (+) refs 35 and 42; (□) refs 37 and 44; (◇) refs 45; (b) (●) ref 32; (■) refs 34 and 35; (×) refs 35 and 43; (◆) refs 37 and 39; (▼) refs 29 and 33. The curves are calculated from eqs 29 and 30.

In fitting the model to the data, weights were assigned to each dataset using our earlier scheme,^{46,47} where

$$\text{wgt} = \text{wgt}(i)[a + b/m_{i,\text{nwt}} + c\sqrt{m_{i,\text{nwt}}}] \quad (24)$$

Values of $\text{wgt}(i)$ for a given dataset are generally inversely related to the influence of that dataset on the model parametrization; for example, datasets with larger values of $\text{wgt}(i)$ carried less influence than those with low values. Datasets were separated by publication, by temperature, and, for the case of isopiestic studies, by standard solution. At temperatures for which multiple datasets exist, the $\text{wgt}(i)$ terms for heat capacity and volumetric data were adjusted to balance datasets so that individual datasets would not bias the temperature dependence of the model through quantity of data. Movement of the model toward data at molalities or temperatures at which only one dataset exists is unavoidable though thermodynamic relationships between the different data types may help to constrain the model's behavior. Values of the constants a , b , and c in eq 24 are listed in Table 2.

Temperature and pressure dependencies of the standard state terms and the adjustable parameters $\beta_{\text{MX}}^{(0)}$, $\beta_{\text{MX}}^{(1)}$, and

Table 2. Parameter Values for Weighting of the Various Data Types in Eq 24 and the Corresponding Molality Ranges over Which Each Weighting Scheme Is Effective^a

$\phi, \text{wgt}(i) = 1.0$			
	$m/m_0 < 0.1$	$0.1 \leq m/m_0 \leq 8$	$m/m_0 > 8$
a	1.0	0.5	1000
$C_{p,\phi}, \text{wgt}(i) = 0.5$			
	$m/m_0 < 0.1$	$0.1 \leq m/m_0 \leq 1$	$m/m_0 > 1$
a	1.0	0.5	0.5
b		0.5	
c	5.0		
$L_\phi, \text{wgt}(i) = 1.0$			
	$m/m_0 < 0.5$	$0.5 \leq m/m_0 \leq 8$	$m/m_0 > 8$
a	0.5	0.1	1000
$V_\phi, \text{wgt}(i) = 3.0$			
	$m/m_0 < 0.7$	$0.7 \leq m/m_0 \leq 8$	$m/m_0 > 8$
a		0.1	1.0
c	0.1		

^a Notable exceptions are as follows. ϕ : Haase et al.,¹⁴ 283 K and 313 K, $\text{wgt}(i) = 1000$; Pearce and Nelson¹² $\text{wgt}(i) = 5.0$; Galkin et al.¹⁸ $\text{wgt}(i) = 100$. $C_{p,\phi}$: 283 K, Hovey et al.⁵ $\text{wgt}(i) = 1.0$; 298 K, Lemire et al.⁷ $\text{wgt}(i) = 1.0$. V_ϕ : $T < 298$ K, $\text{wgt}(i) = 5.0$; 298 K, Partanen et al.;²⁴ Herrington et al.,⁴⁴ Markham,²² and Pearce and Nelson¹² $\text{wgt}(i) = 5.0$; 303 K and 308 K, Partanen et al.²⁴ $\text{wgt}(i) = 50$; 372 K, Lemire et al.⁷ $\text{wgt}(i) = 1.0$.

C_{MX} were confined to the form

$$Q(p_r, T_r) = q_1(T_r) + p_r q_2(T_r) + (\rho_w/\rho_s) q_3(T_r) \quad (25)$$

where

$$q_1(T_r) = a_1/T_r + a_2 + a_3 T_r + a_4 T_r^2 + a_6 \ln T_r \quad (26)$$

$$q_2(T_r) = a_7/T_r + a_8 + a_9 T_r \quad (27)$$

$$q_3(T_r) = a_{19}/T_r + a_{20} + a_{21} T_r \quad (28)$$

$T_r = T/298.15$ K, $p_r = p/100$ MPa, ρ_w = water density, and $\rho_0 = 1$ g cm⁻³. The coefficients of eqs 26–28 for the quantity $\mu^\circ/(RT)$ and for the virial coefficients are listed in Table 3. $C_{p,\phi}^\circ(\text{HClO}_4)$ and $V_\phi^\circ(\text{HClO}_4)$ are derived according to

$$C_{p,\phi}^\circ = [\partial^2(\mu^\circ/RT)/\partial T^2 + (2/T)\partial(\mu^\circ/RT)/\partial T]_p \quad (29)$$

and

$$V_\phi^\circ = [\partial(\mu^\circ/RT)/\partial p]_T \quad (30)$$

For convenience, the fitted forms of $C_{p,\phi}^\circ(\text{HClO}_4)$ and $V_\phi^\circ(\text{HClO}_4)$ are

$$C_{p,\phi}^\circ = (298 \text{ K})^{-2} [6a_4 + a_6 T_r^{-2} + 2a_{21} T_r^{-1} \ln(\rho_w/\rho_0) - 4a_{21}(298 \text{ K})\alpha_p - a_{21}(298 \text{ K})^2 T_r(\partial\alpha_p/\partial T)] \quad (31)$$

$$V_\phi^\circ = a_8/100 + a_{21} T_r \beta_T \quad (32)$$

α_p and β_T refer to water's isobaric expansivity and isothermal compressibility, respectively. The parameters $\beta_{\text{MX}}^{(0)}$, $\beta_{\text{MX}}^{(1)}$, and C_{MX}° are plotted versus temperature in Figure 6. The corresponding derivative forms of the virial coefficients, for example, Q^L , Q^J , and Q^V , are plotted versus temperature in Figure 7. Numerical values of the various thermodynamic quantities and Q_{MX}^i 's (i referring to null, L , J ,

Table 3. Parameter Values for Eqs 25–28^a

a_i	$\mu^\circ(\text{HClO}_4)/(RT)$	$10^3\beta_{\text{HClO}_4}^{(0)}$ kg mol ⁻¹	$\beta_{\text{HClO}_4}^{(1)}$ kg mol ⁻¹	$10^3C_{\text{HClO}_4}$ kg ² mol ⁻²
1		-1.336 534 9 (4.0)	-4.613 649 0 (6.9)	15.858 908 (3.6)
2		3.176 588 1 (4.5)	11.478 882 (8.0)	-12.713 231 (9.3)
3			-9.260 976 1 (9.2)	
4	-5.222 648 0 (2.1)		2.642 013 3 (10.2)	
6	19.325 512 (2.7)			
7		0.509 753 41 (17.1)		
8	2.366 840 8 (0.5)	-0.603 210 78 (14.0)		0.286 343 98 (55.0)
21	-13.283 939 (1.6)			

^a Values in parentheses are percent errors in the estimates for the parameter values.

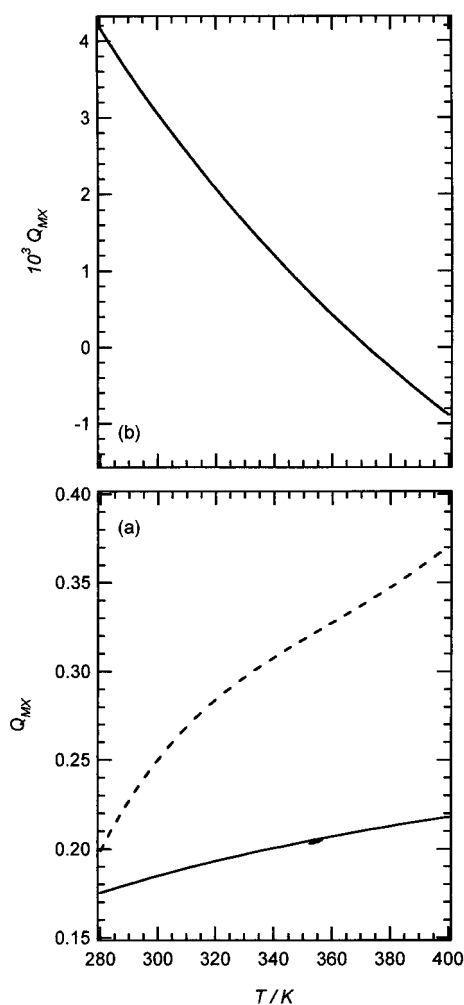


Figure 6. (a) $\beta_{\text{HClO}_4}^{(0)}$ (—), $\beta_{\text{HClO}_4}^{(1)}$ (---), and (b) C_{HClO_4} plotted as functions of temperature.

and V) are tabulated at regular intervals of temperature (and molality for the property values) as Supporting Information available through the American Chemical Society's Web site.

Results and Discussion

The earlier activity coefficient model of Pitzer and Mayorga² was based on the osmotic coefficient tabulations of Robinson and Stokes,⁴⁸ which are, in turn, based on the isopiestic measurements of Robinson and Baker.¹³ While other isopiestic measurements were published after the compilation of Robinson and Stokes, these were apparently not examined. The omission is of no consequence, as all of the isopiestic data are, with the exception of those from Pearce and Nelson,¹² in remarkably good agreement. It was

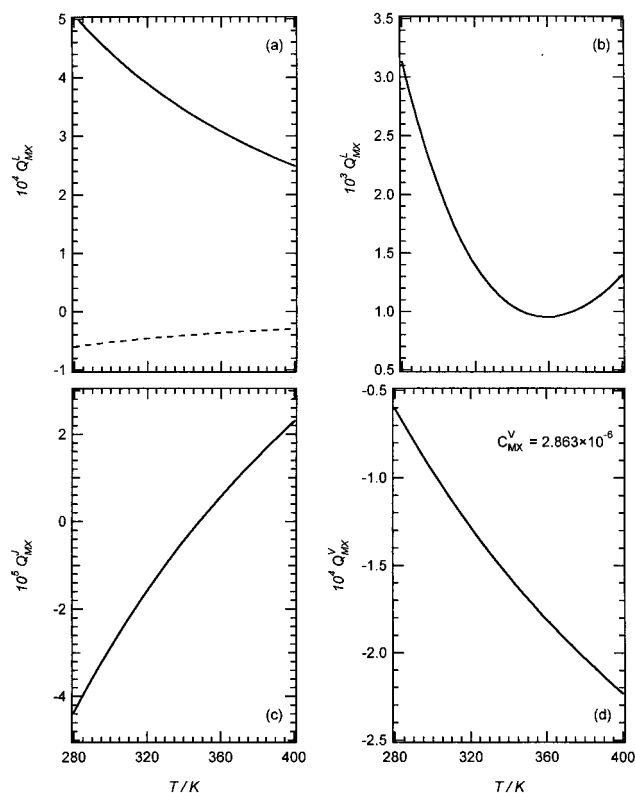


Figure 7. Temperature and pressure derivatives of the interaction parameters (a) $\beta_{\text{HClO}_4}^{(0)L}$ (—) and $C_{\text{HClO}_4}^L$ (---), (b) $\beta_{\text{HClO}_4}^{(1)L}$, (c) $\beta_{\text{HClO}_4}^{(0)J}$, and (d) $\beta_{\text{HClO}_4}^{(0)V}$ plotted against temperature. With the exception of $C_{\text{HClO}_4}^V$, terms not plotted are zero valued.

pointed out in review that we overlooked the dataset of Rush.⁵⁰ The latter data are included in Figure 1; they are in excellent agreement with all data other than those of Pearce and Nelson, and consequently no adjustment was made to the model parameterization. In addition, in the interim between original submission and submission of the revised manuscript, we became aware of an additional set of isopiestic data at 298 K.⁵¹ Considering the quantity and quality of the 298 K isopiestic data used to develop our model, it is doubtful that Mironov's⁵¹ data would provide any improvement. It was also noted in review that our model should be compared to the published electromotive force data^{52–54} (emf; Figure 9). As some of the emf measurements were made at molalities lower than those in the isopiestic experiments and because isopiestic measurements become less reliable at very low molalities, the emf measurements could have better constrained the model in the range between infinite dilution and a few tenths molal. However, Figure 9 illustrates that the model reproduces the data from Mussini et al.⁵² and Torrent et al.⁵³ for $m \leq 0.1$ mol kg⁻¹. At higher molalities the emf data from all

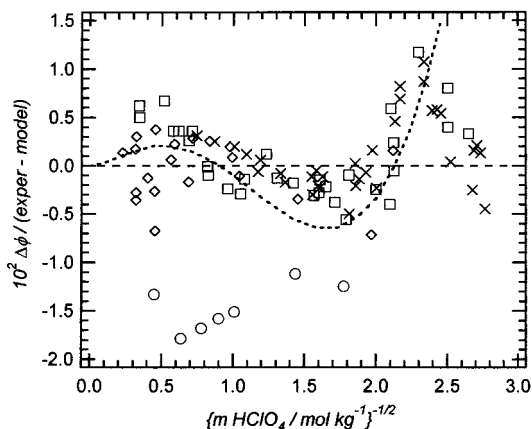


Figure 8. Differences between experimentally measured osmotic coefficients [(○) ref 12; (□) ref 13; (×) refs 15 and 17; (◇) refs 19 and 20] and our model as well as the differences between Pitzer and Mayorga² (---) and our model.

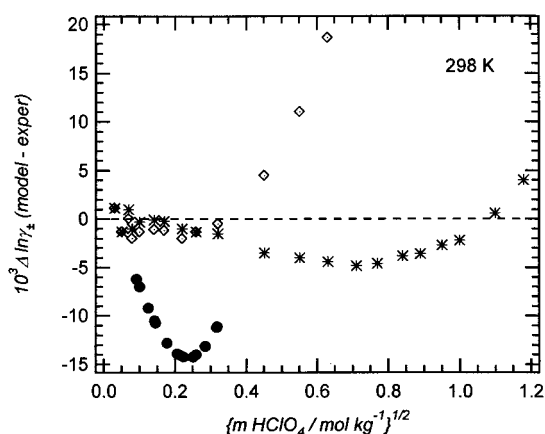


Figure 9. Differences between $\ln \gamma_{\pm}$ derived from our model and from emf measurements [(●) ref 51; (◐) ref 52; (*) ref 53] plotted against $\{(m \text{ HClO}_4)/(\text{mol kg}^{-1})\}^{1/2}$.

three studies^{51–53} have very poor interlaboratory agreement. It should be noted that, in the molality range where all three emf datasets are in disagreement, there are numerous isopiestic data which are in good agreement. Differences between our model and the activity coefficient model of Pitzer-Mayorga² (Figure 8) are within the combined uncertainties of the fits and are probably due to differences in standard solution osmotic coefficients.

The dilution enthalpy measurements fit in this study are the same as those used by Silvester and Pitzer,²⁷ and the results are similar though there are small systematic differences (Figure 10); for example, the Silvester–Pitzer model is uniformly more positive than the tabulated L_{ϕ} values of Vanderzee and Swanson over the full molality range of the fit. The apparent deviation between the Silvester–Pitzer model and the “data” is most likely due to the smoothing procedure used by Vanderzee and Swanson²¹ and is not necessarily an indication of bias in the former model. If this is the case, the consequence is that our model L_{ϕ} values are biased by an average of about 30 J mol^{-1} over the molality range of the fit.

The volumetric data are somewhat interesting in that V_{ϕ} decreases with increasing molality for molalities greater than about 1.0 (Figure 4). In addition, V_{ϕ} changes little over fairly large molality ranges and over the temperature range 298 K to 373 K. The consequence of these features is that an exceptionally simple model is capable of reproducing the data. However, as volumetric models are usually of tertiary

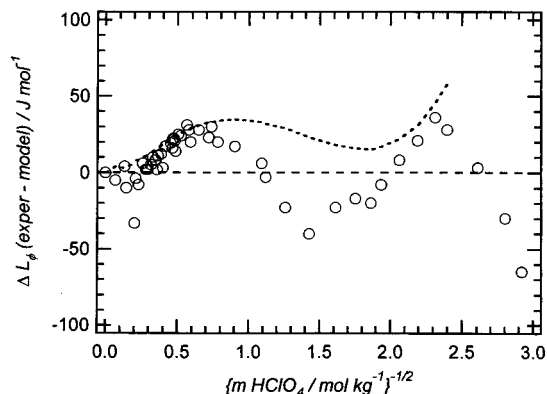


Figure 10. Differences between experimentally measured values of ϕL (○)²¹ and our model as well as differences between Silvester and Pitzer³ (---) and our model.

concern, we will forego further discussion and focus on the heat capacity model.

Three Pitzer ion-interaction models have been fit to the heat capacity data: Lemire et al.,⁷ Criss and Millero,⁴⁹ and Hovey.⁶ The Criss and Millero study utilized only the data from Singh et al.⁹ and consequently is limited to 298 K and $m < 0.4 \text{ mol kg}^{-1}$. Criss and Millero's estimates of $C_{p,\phi}^{\infty}$ vary from $-24 \text{ J mol}^{-1} \text{ K}^{-1}$ to $-27.5 \text{ J mol}^{-1} \text{ K}^{-1}$ depending on which of their tables and electrolyte combinations is used, and their fitted value of $\beta_{\text{MX}}^{(0),J}$ is roughly a factor of 2 more negative than that supported by either Hovey's^{4,5} or Lemire's datasets (discussed below). The various values for $C_{p,\phi}^{\infty}$ obtainable from Criss and Millero do agree with the values supported by the aforementioned datasets. A somewhat reassuring feature of the Criss and Millero study is that our 298 K values of $\beta_{\text{MX}}^{(0),J}$ and $\beta_{\text{MX}}^{(1),J}$ lie squarely on their correlation of the two parameters based on analysis of a large number of aqueous 1:1 electrolyte systems.

Both Lemire et al.⁷ and Hovey⁶ state that their models were fit to both datasets (Hovey also included Singh et al.⁹). Lemire et al.'s $\beta_{\text{MX}}^{(0),J}$ values support this even though their Figure 1 implies the model was fit to only their own data.

While both Criss and Millero and Lemire et al. were able to fit their models to the data using only $\beta_{\text{MX}}^{(0),J}$, Hovey⁶ also included a temperature-dependent C_{MX}^J parameter. Given the level of precision in the data and the fact that the published data do not exist beyond 1.7 m , we believe that inclusion of C_{MX}^J is unwarranted. For example, Figure 3 demonstrates that at 298 K the data are reproduced within the precision of the combined datasets by the Debye–Hückel term and $C_{p,\phi}^{\infty}$ alone. In addition, the sufficiency of $\beta_{\text{MX}}^{(0),J}$ can be demonstrated by omitting C_{MX}^J and rearranging eq 18 as

$$g_{\beta 0} \equiv [C_{p,\phi} / (RT^2) - f^J/m] = C_{p,\phi}^{\infty} / (RT^2) - 2m\beta^{(0),J} \quad (33)$$

and plotting $g_{\beta 0}$ versus molality (Figure 11a–c; f^J refers to the heat capacity form of the Debye–Hückel term defined by eq 19). Figure 11 shows that $g_{\beta 0}$ is linear with molality at all temperatures for which there are data.^{4,5,7} The published values of $\beta_{\text{MX}}^{(0),J}$ from both Lemire and Hovey are similar to those obtainable from Figure 11a. However, values of $C_{p,\phi}^{\infty}$ are somewhat different at $T > 298 \text{ K}$ (Table 4). Note that at 328 K the values of $C_{p,\phi}^{\infty}$ obtainable via eq 33 and Figure 11b are more negative than the published values in Hovey⁶ and Lemire et al.⁷ by as much as $4 \text{ J mol}^{-1} \text{ K}^{-1}$. The only data at 373 K are those of Lemire et al.,⁷

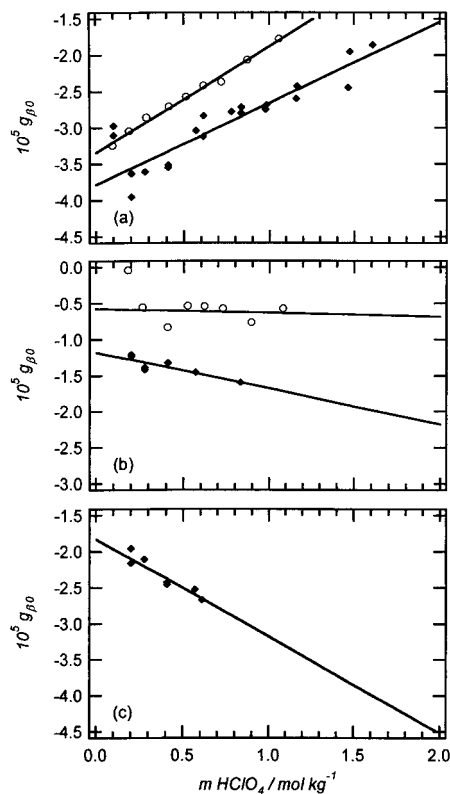


Figure 11. Deviation function $g_{\beta 0}$ (eq 33) based on the heat capacity data at (a) 298 K, (b) 328 K, and (c) 373 K [(○) refs 4 and 5; (◆) ref 7]. Lines are fits to the separate datasets with the data weighted as m^{-1} ; intercepts give $C_{p,\phi}^{\infty}/(RT^2)$, and slopes give $-2\beta_{\text{HClO}_4}^{(0)J}$. See Table 4 for comparisons of $C_{p,\phi}^{\infty}$ and $\beta_{\text{HClO}_4}^{(0)J}$ from eq 33 with previously published values.^{6,7}

Table 4. Comparison of $C_{p,\phi}^{\infty}$ and $\beta_{\text{MX}}^{(0)J}$ Derived from Figures 11a–c with Values from Hovey⁶ and Lemire et al.⁷

ref	$C_{p,\phi}^{\infty}$ J mol ⁻¹ K ⁻¹	$10^6\beta_{\text{HClO}_4}^{(0)J}$ kg mol ⁻¹ K ⁻²	$C_{p,\phi}^{\infty}$ J mol ⁻¹ K ⁻¹	$10^6\beta_{\text{HClO}_4}^{(0)J}$ kg mol ⁻¹ K ⁻²
Figure 11a				
6	-24.7	-7.3	-25.9	-10.7
7	-28.0	-5.6	-27.8	-6.3
Figure 11b				
6	-5.2	0.3	-3.8	2.9
7	-10.6	2.5	-6.4	1.4
Figure 11c				
7	-21.2	6.7	-24.9	4.1

and Figure 11c supports values of $C_{p,\phi}^{\infty}$ and $\beta_{\text{MX}}^{(0)J}$ more positive than the published values.

Through rearrangement of eq 18 as

$$g_{\beta 1} \equiv -[m\{C_{p,\phi}^{\infty}/(RT^2) - C_{p,\phi}^{\infty}/(RT^2)\} - f^J]/2m^2 = \beta_{\text{MX}}^{(0)J} + \beta_{\text{MX}}^{(1)J}g(x) \quad (34)$$

it can be demonstrated that the heat capacity data can also be fit with $\beta_{\text{MX}}^{(1)J}$ (Figure 12a–c). That the intercepts pass through or very near zero demonstrates that the model does not warrant both $\beta_{\text{MX}}^{(0)J}$ and $\beta_{\text{MX}}^{(1)J}$. While arguments can be made for the use of either $\beta_{\text{MX}}^{(0)J}$ or $\beta_{\text{MX}}^{(1)J}$, the choice should not be arbitrary, as it affects the fitted value of $C_{p,\phi}^{\infty}$; for example, it can be seen from eq 34 that $C_{p,\phi}^{\infty}$ and $\beta_{\text{MX}}^{(0)J}$ are not independent if $\beta_{\text{MX}}^{(1)J} \neq 0$. Since $\beta_{\text{MX}}^{(1)J}$ produces somewhat lower residuals and the model behaves more reasonably in extrapolations to higher molalities, we chose to use it rather than $\beta_{\text{MX}}^{(0)J}$.

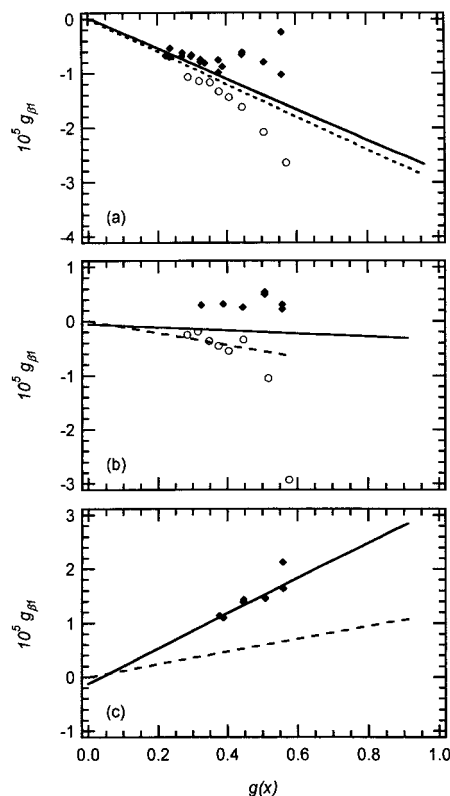


Figure 12. Deviation function $g_{\beta 1}$ plotted against $g(x)$ as defined by eqs 4 and 34. Note that $g(x)$ increases as m decreases [(○) refs 4 and 5; (◆) ref 7]: (a) 298 K, (b) 328 K, (c) 373 K. (—) Isothermal fits to the combined heat capacity data^{4,5,7} with the data weighted as m^{-1} ; intercepts give $\beta_{\text{HClO}_4}^{(0)J}$, and slopes give $\beta_{\text{HClO}_4}^{(1)J}$. For the isothermal fits, values of $\beta_{\text{HClO}_4}^{(0)J}$ are (a) 2.4×10^{-7} , (b) -5.9×10^{-7} , and (c) -1.2×10^{-6} and values of $\beta_{\text{HClO}_4}^{(1)J}$ are (a) -2.8×10^{-5} , (b) -2.8×10^{-6} , and (c) 3.3×10^{-5} . (---) This study, from our polythermal fit to the combined datasets of Table 1; values of $\beta_{\text{HClO}_4}^{(1)J}$ are (a) -3.004×10^{-5} , (b) -1.099×10^{-5} , and (c) 1.184×10^{-5} . Hovey's data cause $\beta_{\text{HClO}_4}^{(1)J}$ to be more negative than if guided only by Lemire's data, and our model at 373 K is consistent with this tendency (e.g., compare range of values obtainable from respective studies per this figure with Figure 7c).

We believe that both the Lemire⁷ and Hovey⁶ heat capacity models are overfit in their temperature dependencies. Both of the former models use a temperature dependence for the adjustable parameters of the form

$$Q^J = c_1 + c_2/(T - \text{const}) + c_3T \quad (35)$$

where const refers to 190 K for Hovey⁶ and 0 K for Lemire⁷ and c_3 is nonzero in both models. This form requires a T^3 dependence on $\beta_{\text{MX}}^{(0)}$ in eqs 5, 8, and 9 while other systems such as HCl(aq)³⁰ and KCl(aq)³⁴ show nearly linear or T^{-1} dependencies on $\beta_{\text{MX}}^{(0)}$ in this temperature range; $\beta_{\text{MX}}^{(0)}$ for NaCl(aq) does not have a cubic form below about 523 K.²⁹

Finally, it is interesting to note that our model reproduces the heat capacity data with five fit parameters versus nine in the Hovey⁶ model and six in Lemire's⁷ model. Note that our a_1 terms cancel in eqs 20b–c, leaving only the a_4 , a_6 , and a_{21} terms in $C_{p,\phi}^{\infty}$ and the a_3 and a_4 terms in $\beta_{\text{MX}}^{(1)J}$ such that $\beta_{\text{MX}}^{(1)J} = 298^{-2}(2q_3/T_r + 6q_4)$. In addition, our model reproduces both the activity coefficient and derivative property data with a total of 15 fit parameters versus 30 in the Hovey⁶ model, which reproduces only the heat capacity and volumetric data.

Conclusion

At $m \leq 6 \text{ mol kg}^{-1}$ and temperatures near 298 K, our model is not substantially different from the Pitzer–Mayorga² and Silvester–Pitzer²⁷ activity coefficient and enthalpy models. The significant contribution of this study is made through the inclusion of a larger array of activity coefficient and derivative property data (e.g. enthalpy, heat capacity, and volumetric) into a self-consistent model which reproduces the aqueous phase thermodynamic data over the full range of temperatures and pressures at which data currently exist. This study also serves to illustrate that additional thermodynamic measurements, particularly derivative property measurements, are warranted for this system. Consequently, it is anticipated that our model will eventually be obviated though this study should serve as a useful guide to subsequent experimental work and thermochemical model development for this system.

Supporting Information Available:

Tables of numerical values of the various thermodynamic quantities and Q_{MX}^i 's (i referring to null, L , J , and V) tabulated at regular intervals of temperature (and molality for the property values). This material is available free of charge via the Internet at <http://pubs.acs.org>.

Literature Cited

- Hamer, W. J.; Wu, Y.-C. Osmotic coefficients and mean activity coefficients of uni-valent electrolytes in water at 25 °C. *J. Phys. Chem. Ref. Data* **1972**, *1*, 1047–1099.
- Pitzer, K. S.; Mayorga, G. Thermodynamics of electrolytes. II. Activity and osmotic coefficients for strong electrolytes with one or both ions univalent. *J. Phys. Chem.* **1973**, *77*, 2300–2308.
- Silvester, L. F.; Pitzer, K. S. Thermodynamics of electrolytes. X. Enthalpy and the effect of temperature on the activity coefficients. *J. Solution Chem.* **1978**, *7*, 327–337.
- Hovey, J. K.; Hepler, L. G.; Tremaine, P. R. Apparent molar heat capacities and volumes of aqueous HClO_4 , HNO_3 , $(\text{CH}_3)_4\text{NOH}$ and K_2SO_4 at 298.15 K. *Thermochim. Acta* **1988**, *126*, 245–253.
- Hovey, J. K.; Hepler, L. G. Apparent and partial molar heat capacities and volumes of aqueous HClO_4 and HNO_3 from 10 to 55 °C. *Can. J. Chem.* **1989**, *67*, 1489–1495.
- Hovey, J. K. Thermodynamics of hydration of a 4+ aqueous ion: Partial molar heat capacities and volumes of aqueous thorium(IV) from 10 to 55 °C. *J. Phys. Chem. B* **1997**, *101*, 4321–4334.
- Lemire, R. J.; Campbell, A. B.; Pan, P. Apparent molar heat capacities and volumes for $\text{HClO}_4(\text{aq})$ to 373 K. *Thermochim. Acta* **1996**, *286*, 225–231.
- Pogue, R.; Atkinson, G. Apparent molal volumes and heat capacities of aqueous hydrogen chloride and perchloric acid at 15–55 °C. *J. Chem. Eng. Data* **1988**, *33*, 495–499.
- Singh, P. P.; McCurdy, K. G.; Woolley, E. M.; Hepler, L. G. Heat capacities of aqueous perchloric acid and sodium perchlorate at 298 K: ΔC_p° of ionization of water. *J. Solution Chem.* **1977**, *6*, 327–330.
- Pitzer, K. S. Thermodynamics of electrolytes. I. Theoretical basis and general equations. *J. Phys. Chem.* **1973**, *77*, 268–277.
- Pitzer, K. S. Ion interaction approach: theory and data correlation. In *Activity Coefficients in Electrolyte Solutions*, 2nd ed.; CRC Press: Boca Raton, FL, 1991.
- Pearce, J. N.; Nelson, A. F. The vapor pressures and activity coefficients of aqueous solutions of perchloric acid at 25 °C. *J. Am. Chem. Soc.* **1933**, *55*, 3075–3081.
- Robinson, R. A.; Baker, O. J. The vapour pressures of perchloric acid solutions at 25 °C. *Trans. R. Soc. N. Z.* **1946**, *76*, 250–254.
- Haase, R.; Dücker, K.-H.; Küppers, H. A. Aktivitätskoeffizienten und dissoziationskonstanten wässriger salpetersäure und überchlorsäure. *Ber. Bunsen-Ges. Phys. Chem.* **1965**, *69*, 97–109.
- Rush, R. M.; Johnson, J. S. Isopiestic measurements of the osmotic and activity coefficients for the systems $\text{HClO}_4\text{--LiClO}_4\text{--H}_2\text{O}$, $\text{HClO}_4\text{--NaClO}_4\text{--H}_2\text{O}$, and $\text{LiClO}_4\text{--NaClO}_4\text{--H}_2\text{O}$. *J. Phys. Chem.* **1968**, *72*, 767–774.
- Wai, H.; Yates, K. Determination of the activity of water in highly concentrated perchloric acid solutions. *Can. J. Chem.* **1969**, *47*, 2326–2328.
- Rush, R. M.; Johnson, J. S. Isopiestic measurements of the osmotic and activity coefficients for the systems $\text{HClO}_4 + \text{UO}_2(\text{ClO}_4)_2 + \text{H}_2\text{O}$ and $\text{NaClO}_4 + \text{UO}_2(\text{ClO}_4)_2 + \text{H}_2\text{O}$ at 25 °C. *J. Chem. Thermodyn.* **1971**, *3*, 779–793.
- Galkin, V. I.; Lilich, L. S.; Kurbanova, Z. I.; Chernykh, L. V. Vapor pressure of water in perchloric acid–water and metal perchlorate–water systems at 0 and 50 °C. *Zh. Fiz. Khim.* **1973**, *37*, 443–444.
- Boyd, G. E. Solute activity coefficients in dilute aqueous electrolyte mixtures. III. The ternary system $\text{HClO}_4 + \text{UO}_2(\text{ClO}_4)_2 + \text{H}_2\text{O}$ at 25 °C. *Inorg. Chem.* **1977**, *11*, 747–756.
- Boyd, G. E. Osmotic and activity coefficients of aqueous HTcO_4 and HReO_4 solutions at 25 °C. *Inorg. Chem.* **1978**, *17*, 1808–1810.
- Vanderzee, C. E.; Swanson, J. A. Heats of dilution and relative apparent molal enthalpies of aqueous sodium perchlorate and perchloric acid. *J. Phys. Chem.* **1963**, *67*, 285–291.
- Markham, A. E. Density of perchloric acid solutions. *J. Am. Chem. Soc.* **1941**, *63*, 874.
- Herrington, T. M.; Pethybridge, A. D.; Roffey, M. G. Densities of hydrochloric, hydrobromic, hydriodic, and perchloric acids from 25 to 75 °C at 1 atm. *J. Chem. Eng. Data* **1985**, *30*, 264–267.
- Partanen, J. I.; Juusola, P. M. Density of aqueous perchloric acid solutions in the molality range 0–4.4 mol kg^{-1} at 293.15, 298.15, 303.15, and 308.15 K. *Acta Chem. Scand.* **1993**, *47*, 338–343.
- Hill, P. G. A unified fundamental equation for the thermodynamic properties of H_2O . *J. Phys. Chem. Ref. Data* **1990**, *19*, 1233–1274.
- Archer, D. G.; Wang, P. The dielectric constant of water and Debye–Hückel limiting law slopes. *J. Phys. Chem. Ref. Data* **1990**, *19*, 371–411.
- Silvester, L. F.; Pitzer, K. S. Thermodynamics of electrolytes. 8. High-temperature properties, including enthalpy and heat capacity, with application to sodium chloride. *J. Phys. Chem.* **1977**, *81*, 1822–1828.
- Rard, J. A.; Habenschuss, A.; Spedding, F. H. A review of the osmotic coefficients of aqueous H_2SO_4 at 25 °C. *J. Chem. Eng. Data* **1976**, *21*, 374–379.
- Archer, D. G. Thermodynamic properties of the $\text{NaCl} + \text{H}_2\text{O}$ system II. Thermodynamic properties of $\text{NaCl}(\text{aq})$, $\text{NaCl}\cdot 2\text{H}_2\text{O}(\text{cr})$, and phase equilibria. *J. Phys. Chem. Ref. Data* **1992**, *21*, 793–829.
- Holmes, H. F.; Busey, R. H.; Simonson, J. M.; Mesmer, R. E.; Archer, D. G.; Wood, R. H. The enthalpy of dilution of $\text{HCl}(\text{aq})$ to 648 K and 40 MPa: Thermodynamic properties. *J. Chem. Thermodyn.* **1987**, *19*, 863–890.
- Sharygin, A. V.; Wood, R. H. Volumes and heat capacities of aqueous solutions of hydrochloric acid at temperatures from 298.15 K to 623 K and pressures to 28 MPa. *J. Chem. Thermodyn.* **1997**, *29*, 125–148.
- Mastroianni, M.; Criss, C. M. Standard partial molal heat capacities of sodium perchlorate in water from 0 to 90 °C and in anhydrous methanol from –5–55 °C. *J. Chem. Eng. Data* **1972**, *17*, 222–226.
- Roux, A.; Musbally, G. M.; Perron, G.; Desnoyers, J. E.; Singh, P. P.; Woolley, E. M.; Hepler, L. G. Apparent molal heat capacities and volumes of aqueous electrolytes at 25 °C: NaClO_3 , NaClO_4 , NaNO_3 , NaBrO_3 , NaIO_3 , KClO_3 , KBrO_3 , KIO_3 , NH_4NO_3 , NH_4Cl , and NH_4ClO_4 . *Can. J. Chem.* **1978**, *56*, 24–28.
- Archer, D. G. Thermodynamic properties of the $\text{KCl} + \text{H}_2\text{O}$ System. *J. Phys. Chem. Ref. Data* **1999**, *28*, 1–17.
- Saluja, P. P. S.; Pitzer, K. S.; Phutela, R. C. High-temperature thermodynamic properties of several 1:1 electrolytes. *Can. J. Chem.* **1986**, *64*, 1328–1335.
- Kelley, K. K. Contributions to the data on theoretical metallurgy XIII. High-temperature heat-content, heat-capacity, and entropy data for the elements and inorganic compounds. *U. S. Bur. Mines Bull.* **1960**, *584*.
- Pan, P.; Campbell, A. B. Apparent and standard molar volumes and heat capacities of aqueous $\text{Ni}(\text{ClO}_4)_2$ from 25 to 85 °C. *J. Solution Chem.* **1997**, *26*, 461–478.
- Spitzer, J. J.; Singh, P. P.; McCurdy, K. G.; Hepler, L. G. Apparent molar heat capacities and volumes of aqueous electrolytes: CaCl_2 , $\text{Cd}(\text{NO}_3)_2$, CoCl_2 , $\text{Cu}(\text{ClO}_4)_2$, $\text{Mg}(\text{ClO}_4)_2$, and NiCl_2 . *J. Solution Chem.* **1978**, *7*, 81–86.
- Perron, G.; Roux, A.; Desnoyers, J. E. Heat capacities and volumes of NaCl , MgCl_2 , CaCl_2 , and NiCl_2 up to 6 molal in water. *Can. J. Chem.* **1981**, *59*, 3049–3054.
- Smith-Magowan, D.; Wood, R. H.; Tillett, D. M. Heat capacities of aqueous solutions of nickelous chloride and nickel chloridesodium chloride ($\text{NiCl}_2\cdot 2\text{NaCl}$) from 0.12 to 3.0 mol kg^{-1} and 321 to 572 K at a pressure of 17.7 MPa. *J. Chem. Eng. Data* **1982**, *27*, 335–42.
- Ellis, A. J. Partial molal volumes in high-temperature water: Part III. Halide and oxyanion salts. *J. Chem. Soc. (A)* **1968**, 1138–1143.
- Pabalan, R. T.; Pitzer, K. S. Apparent molar heat capacity and other thermodynamic properties of aqueous KCl solutions to high temperatures and pressures. *J. Chem. Eng. Data* **1988**, *33*, 354–362.
- Saluja, P. P. S.; Lemire, R. J.; LeBlanc, J. C. High-temperature thermodynamics of aqueous alkali-metal salts. *J. Chem. Thermodyn.* **1992**, *24*, 181–203.

- (44) Herrington, T. M.; Roffey, M. G.; Smith, D. P. Densities of aqueous electrolytes MnCl_2 , CoCl_2 , NiCl_2 , ZnCl_2 , and CdCl_2 from 25 to 72 °C at 1 atm. *J. Chem. Eng. Data* **1986**, *31*, 221–225.
- (45) Pogue, R. F.; Atkinson, G. The volume of ions and ion–solvent pair correlation functions. *Int. J. Thermophys.* **1988**, *9*, 689–702.
- (46) Sterner, S. M.; Felmy, A. R.; Oakes, C. S.; Pitzer, K. S. Correlation of thermodynamic data for aqueous electrolyte solutions to very high ionic strength using INSIGHT: Vapor saturated water activity in the system $\text{CaCl}_2\text{--H}_2\text{O}$ to 250 °C and solid saturation. *Int. J. Thermophys.* **1998**, *19*, 761–770.
- (47) Oakes, C. S.; Felmy, A. R.; Sterner, S. M. Thermodynamic properties of aqueous calcium nitrate [$\text{Ca}(\text{NO}_3)_2$] to the temperature of 373 K including new enthalpy of dilution data. *J. Chem. Thermodyn.* **2000**, *32*, 29–54.
- (48) Robinson, R. A.; Stokes, R. H. *Electrolyte Solutions. The Measurement and Interpretation of Conductance, Chemical Potential and Diffusion in Solutions of Simple Electrolytes*; Butterworth Scientific Publications: London, 1959.
- (49) Criss, C. M.; Millero, F. J. Modeling the heat capacities of aqueous 1–1 electrolyte solutions with Pitzer's equations. *J. Phys. Chem.* **1996**, *100*, 1288–1294.
- (50) Rush, R. M. Isopiestic measurements of the osmotic and activity coefficients for the system $\text{HClO}_4\text{--Ba}(\text{ClO}_4)_2\text{--H}_2\text{O}$ at 25 °C. *J. Chem. Eng. Data* **1986**, *31*, 478–481.
- (51) Mironov, I. V.; Sokolova, N. R.; Makotchenko, E. V. Activities of the components in the chloroauric acid–perchloric acid–water system. *Zh. Fiz. Khim.* **1999**, *73*, 1977–1982.
- (52) Covington, A. K.; Prue, J. E. Activity coefficients of nitric and perchloric acids in dilute aqueous solution from emf and transport-number measurements. *J. Chem. Soc.* **1957**, 1567–1572.
- (53) Mussini, T.; Galli, R.; Dubini-Paglia, E. Use of perchlorate-responsive membrane cell for the determination of activity coefficients of aqueous perchloric acid. *Trans. Faraday Soc.* **1972**, *68*, 1322–1327.
- (54) Torrent, J.; Sanz, F.; Virgili, J. Activity coefficients of aqueous perchloric acid. *J. Solution Chem.* **1986**, *15*, 363–375.

Received for review February 11, 2000. Accepted March 27, 2001. This research was conducted at the Pacific Northwest National Laboratory, operated by Battelle for the U. S. Department of Energy (DOE) under contract DE-AC06-76RLO 1830, in collaboration with Japan Nuclear Cycle Development Institute (JNC) under agreement with DOE for the project "Development of Fundamental Thermodynamic and Adsorption Data".

JE000051B